J|A|C|S
ARTICLES
Published on Web 08/07/2003

Kinetics and Mechanism of the Proton Transfer to Cp*Fe(dppe)H: Absence of a Direct Protonation at the Metal Site

Natalia V. Belkova,[†] Pavel O. Revin,[†] Lina M. Epstein,[†] Evgenii V. Vorontsov,[†] Vladimir I. Bakhmutov,[†,§] Elena S. Shubina,*[,†] Edmond Collange,[‡] and Rinaldo Poli*[,‡]

Contribution from the Nesmeyanov Institute of Organoelement Compounds, Russian Academy of Sciences, Vavilov Street 28, 119991 Moscow, Russia, and Laboratoire de Synthèse et d'Electrosynthèse Organométalliques (LSEO UMR 5632), Université de Bourgogne, Faculté de Sciences "Gabriel", 6 boulevard Gabriel, 21000 Dijon, France

Received April 29, 2003; E-mail: poli@u-bourgogne.fr

Abstract: The reaction between Cp*Fe(dppe)H and a number of different proton donors (2-fluoroethanol, MFE; 2,2,2-trifluoroethanol, TFE; hexafluoro-2-propanol, HFIP; perfluoro-*tert*-butyl alcohol, PFTB; and trifluoroacetic acid, TFA) has been investigated spectroscopically by variable-temperature infrared, UV−visible, and NMR spectroscopy, and has been measured kinetically by the stopped-flow technique with UV−visible detection. The low-temperature IR study shows the establishment of hydrogen-bonding interactions which involve the hydride ligand as the proton accepting site. This investigation quantifies the thermodynamics of the hydrogen-bonding interaction and the basicity factor (E_i) of the hydride complex. All techniques agree in indicating an equilibration process, after the immediate hydrogen-bond formation, between the hydride complex and an intermediate dihydrogen complex, $[Cp^*Fe(dppe)(H_2)]^+$. The equilibrium is shifted toward the dihydrogen complex to a greater extent for the stronger alcohols and for higher alcohol/Fe ratios. The observed equilibration rate constant is linearly dependent on the alcohol concentration, in agreement with the involvement of two alcohol molecules and the formation of a homoconjugate pair. The rate constant increases with the acidity of the proton donor (TFE < HFIP < PFTB < TFA). The rate of the subsequent irreversible isomerization leading to the classical dihydride complex, $[Cp^*Fe(dppe)H_2]^+$, is first order, and the rate constant does not depend on the proton donor nature. The reaction continues, if conducted in CH_2Cl_2, with a third, slower step leading to the paramagnetic $[Cp^*Fe(dppe)Cl]^+$ product. The kinetic data are in accord with an isomerization mechanism consisting of an intramolecular reorganization, leading in one step from the dihydrogen complex to the classical dihydride species, and disagree with the occurrence of a proton-transfer process at the metal site.

Introduction

Proton-transfer processes to and from transition metal centers and hydride ligand sites are key steps in many stoichiometric and catalytic chemical and biochemical processes and have received a great deal of attention over the last two decades.[1] While protonation of a metal site affords a new hydride ligand, proton transfer to a hydride ligand site affords a dihydrogen ligand (nonclassical dihydride complex, or σ-H_2 complex), see Scheme 1.

A fundamental issue is that of the thermodynamic versus kinetic acidity, whereby nonclassical hydride complexes (**III**) are shown to be deprotonated faster than the classical tautomers (**VI**), even when the latter are stronger acids in the thermodynamic sense.[2] The reverse process, protonation of a hydride complex, is correspondingly faster at a hydride ligand site relative to the metal lone pair (hydride ligands are, in general, kinetically more basic than transition metal centers).[3,4] Indeed, dihydrogen complexes have often been detected as intermediates along the formation of classical polyhydrides as the thermodynamically stable final products.[5−9]

Another impetus to this area has been given by the discovery of "nonclassical dihydrogen bonding"; that is, adducts of type **I** are shown to be intermediates along the proton-transfer

[†] Russian Academy of Sciences.
[‡] Université de Bourgogne.
[§] Current address: Department of Chemistry, Texas A&M University, P.O. Box 30012, College Station, TX 77842-3012.

(1) Peruzzini, M., Poli, R., Eds. *Recent Advances in Hydride Chemistry*; Elsevier: Amsterdam, 2001.
(2) Kristjánsdóttir, S. S.; Norton, J. R. In *Transition Metal Hydrides*; Dedieu, A., Ed.; VCH: New York, 1992; pp 309−359.
(3) Papish, E. T.; Rix, F. C.; Spetseris, N.; Norton, J. R.; Williams, R. D. *J. Am. Chem. Soc.* **2000**, *122*, 12235−12242.
(4) Papish, E. T.; Magee, M. P.; Norton, J. R. In *Recent Advances in Hydride Chemistry*; Peruzzini, M., Poli, R., Eds.; Elsevier: Amsterdam, 2001; pp 39−74.
(5) Parkin, G.; Bercaw, J. E. *J. Chem. Soc., Chem. Commun.* **1989**, 255−257.
(6) Chinn, M. S.; Heinekey, D. M. *J. Am. Chem. Soc.* **1990**, *112*, 5166−5175.
(7) Jia, G.; Lough, A. J.; Morris, R. H. *Organometallics* **1992**, *11*, 161−171.
(8) Hamon, P.; Toupet, L.; Hamon, J.-R.; Lapinte, C. *Organometallics* **1992**, *11*, 1429−1431.
(9) Hamon, J. R.; Hamon, P.; Toupet, L.; Costuas, K.; Saillard, J. Y. C. R. *Acad. Sci., Ser. IIc: Chim.* **2002**, *5*, 89−98.

10.1021/ja0358450 CCC: $25.00

Scheme 1

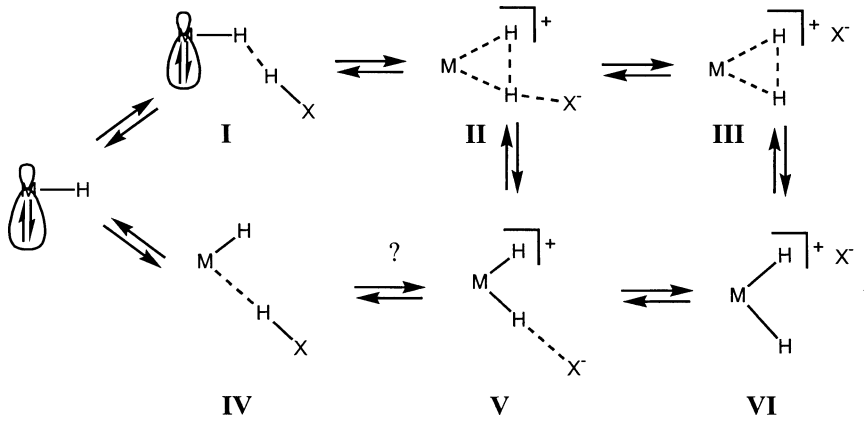

pathway to and from dihydrogen complexes. The latter may exist as either free complexes, **III**, or retain the conjugate base in a hydrogen-bonding interaction, **II**. Systems such as **I** have also been shown to be intermediates along the pathway to the heterolytic splitting of dihydrogen.[10] Depending on the relative strength of the proton donor and acceptor, these can be stable entities in solution, displaying characteristic spectroscopic signatures.[11,12] The proton transfer to the metal site can analogously be imagined as proceeding via a hydrogen-bonded intermediate **IV**, leading to either free (**VI**) or hydrogen-bonded (**V**) classical hydride product. A number of studies of adducts such as **IV** are available,[13] and the general implication is that they are indeed intermediates in the proton-transfer process. However, the interconversion between classical and nonclassical tautomers takes place rather easily in many cases and can in principle occur both on the free (**III** and **VI**) and on the hydrogen-bonded (**II** and **V**) complexes, thus opening a second possible pathway for protonation of the metal center (fast protonation of the hydride site followed by isomerization).

Hydrogen-bonded complexes such as **IV** and **V** have been located along the pathway of proton transfer to the metal center when no other hydride ligands are present,[14−19] but only in a few cases have these been proven intermediates of the direct proton transfer to the metal site.[20−23] Norton has recently shown that the rate of metal protonation in compound $CpW(CO)_2(PMe_3)H$ is 9.6 times smaller than the rate of hydride protonation. The rate of metal protonation was obtained indirectly from the combination of the measured deprotonation rate of the classical dihydride complex $CpW(CO)_2(PMe_3)H_2^+$ and the measured pK_a value. It is quite possible, however, that the deprotonation reaction occurs only after isomerization to the nonclassical intermediate. Thus, the 9.6 factor between these two rates could merely be related to the tautomerization thermodynamics and does not imply the occurrence of a direct metal protonation. More detailed information would only be available from an independent analysis of the tautomerization kinetics or equilibria, but, unfortunately, the nonclassical tautomer cannot be directly observed for this system.

Previous work by other authors has addressed specific aspects of the kinetics and mechanism of proton transfer to a hydride complex. The work of Basallote et al. mostly concerns the formation of dihydrogen complexes that do not evolve to the classical isomers but rather to H_2 substitution products, such as $[MH(H_2)L_4]^+$ (M = Fe, Ru; L = P-donor ligand).[24−27] A single exception is the formation of complexes $[CpRuL_2(H_2)]^+$ (L_2 = dppm, dppe, and $(PPh_3)_2$) which further evolve to the classical isomers, but the kinetics investigation was not extended to this isomerization step.[28] Work by Chinn and Heinekey on the protonation of a variety of CpRuH(L)(L′) and related Cp* complexes,[6] and the later extension to related systems by Puerta et al.,[29] on the other hand, address the mechanism of the reversible or irreversible conversion of the dihydrogen complexes to the corresponding dihydrides. Although the low-temperature protonation was shown to occur selectively at the hydride site for these systems, the results of those studies cannot exclude a competitive protonation of the metal site at ambient temperature.

To shine more light onto this basic question, we have decided to carry out detailed investigations on the proton transfer to complex Cp*Fe(dppe)H, prepared several years ago by Hamon et al.[8,9] A selective protonation at the hydride site with formation

(10) Morris, R. H. In *Recent Advances in Hydride Chemistry*; Peruzzini, M., Poli, R., Eds.; Elsevier: Amsterdam, 2001; pp 1−38.
(11) Epstein, L. M.; Belkova, N. V.; Shubina, E. S. In *Recent Advances in Hydride Chemistry*; Peruzzini, M., Poli, R., Eds.; Elsevier: Amsterdam, 2001; pp 391−418.
(12) Epstein, L. M.; Shubina, E. S. *Coord. Chem. Rev.* **2002**, *231*, 165−181.
(13) Shubina, E. S.; Belkova, N. V.; Epstein, L. M. *J. Organomet. Chem.* **1997**, *536−537*, 17−29.
(14) Kazarian, S. G.; Hamley, P. A.; Poliakoff, M. *Chem. Commun.* **1992**, 994−997.
(15) Kazarian, S. G.; Hamley, P. A.; Poliakoff, M. *J. Am. Chem. Soc.* **1993**, *115*, 9069−9079.
(16) Poliakoff, M.; Howdle, S. M.; Kazarian, S. G. *Angew. Chem., Int. Ed. Engl.* **1995**, *34*, 1275−1295.
(17) Shubina, E. S.; Krylov, A. N.; Kreindlin, A. Z.; Rybinskaya, M. I.; Epstein, L. M. *J. Mol. Struct.* **1993**, *301*, 1−5.
(18) Shubina, E. S.; Krylov, A. N.; Muratov, D. V.; Filchikov, A. A.; Epstein, L. M. *Russ. Chem. Bull.* **1993**, *42*, 1919−1920.
(19) Epstein, L. M.; Krylov, A. N.; Shubina, E. S. *J. Mol. Struct.* **1994**, *322*, 345−352.
(20) Shubina, E. S.; Krylov, A. N.; Belkova, N. V.; Epstein, L. M.; Borisov, A. P.; Mahaev, V. D. *J. Organomet. Chem.* **1995**, *493*, 275−277.
(21) Albinati, A.; Bakhmutov, V. I.; Belkova, N. V.; Bianchini, C.; de los Rios, I.; Epstein, L.; Gutsul, E. I.; Marvelli, L.; Peruzzini, M.; Rossi, R.; Shubina, E. S.; Vorontsov, E. V.; Zanobini, F. *Eur. J. Inorg. Chem.* **2002**, 1530−1539.
(22) Hascall, T.; Baik, M. H.; Bridgewater, B. A.; Shin, J. H.; Churchill, D. G.; Friesner, R. A.; Parkin, G. *Chem. Commun.* **2002**, 2644−2645.
(23) Belkova, N. V.; Gutsul, E. I.; Epstein, L.; Shubina, E. S.; Bianchini, C.; Zanobini, F.; Peruzzini, M., unpublished observations.
(24) Basallote, M. G.; Durán, J.; Fernández-Trujillo, M. J.; Máñez, M. A.; de la Torre, J. R. *J. Chem. Soc., Dalton Trans.* **1998**, 745−750.
(25) Basallote, M. G.; Durán, J.; Fernández-Trujillo, M. J.; Máñez, M. A. *J. Chem. Soc., Dalton Trans.* **1998**, 2205−2210.
(26) Basallote, M. G.; Durán, J.; Fernández-Trujillo, M. J.; Máñez, M. A. *Inorg. Chem.* **1999**, *38*, 5067−5071.
(27) Basallote, M. G.; Durán, J.; Fernández-Trujillo, M. J.; Máñez, M. A. *J. Organomet. Chem.* **2000**, *609*, 29−35.
(28) Basallote, M. G.; Durán, J.; Fernández-Trujillo, M. J.; Máñez, M. A. *Organometallics* **2000**, *19*, 695−698.
(29) de los Ríos, I.; Jiménez-Tenorio, M.; Padilla, J.; Puerta, M. C.; Valerga, P. *Organometallics* **1996**, *15*, 4565−4574.

of the dihydrogen complex as an observable intermediate and the thermodynamic preference for the metal site were established by using the strong acid HBF_4. Thus, the protonation at the hydride site and the isomerization can be analyzed independently from the kinetic and thermodynamic points of view *at the same temperature*. Our study was carried out by using the following proton donors (HA), in order of increasing acid strength: 2-monofluoroethanol (MFE), 2,2,2-trifluoroethanol (TFE), hexafluoro-2-propanol (HFIP), perfluoro-*tert*-butyl alcohol (PFTB), and trifluoroacetic acid (TFA). The interaction has been investigated by a combination of NMR, IR, and UV−visible spectroscopy at various temperatures in the 200−290 K range. This approach allowed us to study the overall process step by step. The proton transfer and isomerization rates at room temperature have been determined by both classical mixing and rapid mixing (stopped-flow) techniques. This is the first reported study where an independent kinetic analysis is carried out for both the proton transfer and the isomerization steps, and the first study of this kind where proton donors of different acid strength are used and compared.

Experimental Section

All manipulations were carried out under an argon atmosphere by standard Schlenk techniques. The Cp*Fe(dppe)H hydride was synthesized according to the literature.[30]

IR and UV−Visible Investigations. The IR measurements were performed on a "Specord M82" spectrometer (IR) on 0.1−0.15 M (for the ν(OH) measurements) or 0.02−0.025 M (for the ν(MH) measurements) hydride solutions in CH_2Cl_2 (0.12 cm path length) using CaF_2 cells. UV measurements were performed on Specord M-40 and Varian Cary 5 spectrophotometers on 0.01 M solutions in CH_2Cl_2. All IR and UV measurements were carried out by use of a home-modified cryostat (Carl Zeiss Jena) in the 200−290 K temperature range. The cryostat modification allows the transfer of the reagents (premixed either at low or room temperature) directly into the cell under an inert atmosphere and at the desired temperature. The accuracy of the temperature adjustment was ±0.5 K. This setup was used both for the variable-temperature equilibrium studies and for the kinetics investigations at constant temperature with UV−visible spectroscopic monitoring. An IR study was also attempted in cyclohexane. However, the precipitation of the cationic dihydrogen complex rendered impossible a careful investigation in this solvent.

NMR Investigations. The NMR studies were carried out in standard 5 mm-NMR tubes containing solutions of the complexes in CD_2Cl_2. The ^{1}H and ^{31}P NMR data were collected with a Bruker AMX 400 spectrometer operating at 400.13 and 161.98 MHz, respectively. The conventional inversion−recovery method (180−τ−90) was used to determine the variable-temperature longitudinal relaxation time T_1. The calculation of the relaxation times was made using the nonlinear three-parameter fitting routine of the spectrometers. In each experiment, the waiting period was 5 times larger than the expected relaxation time, and 16−32 variable delays were employed. The duration of the pulses was controlled at every temperature. Low-temperature experiments were carried out in the 180−260 K temperature range using a TV-3000 Bruker temperature unit. The accuracy and stability of temperature were ±1 K. All mixings between the alcohols and the hydride complexes were performed at low temperature.

Stopped-Flow Investigations. The stopped-flow kinetic runs were carried out at 25 °C with a Hitech SF-61-DX2 apparatus coupled to a Hitech diode-array UV−visible spectrophotometer. Given the extreme air-sensitivity of the hydride compound, unacceptable results were obtained at the low concentrations required for work in a suitable absorbance range when using a regular 1 cm cell (ca. 5×10^{-4} M). This phenomenon is attributed to oxidation by oxygen diffusion through the instrument transfer lines, as confirmed by the observation of small and irreproducible signal evolutions when shooting the same hydride solution from both syringes. Switching to a 10-fold concentration and to a smaller path length (1.5 mm) reduced the oxidation problem below acceptable noise levels. Only the data that were collected within the first 50 s were analyzed, yielding reproducible results. No oxidation problems were evident, on the other hand, for the experiments carried out by the more traditional long time scale monitoring. Data analyses were carried out by using the SPECFIT[31] global analysis package of programs.

Table 1. IR (νFe−H), ^{1}H (Hydride Resonance), and ^{31}P NMR Data in CD_2Cl_2 for Cp*Fe(dppe)H and for the Products Deriving from Its Interaction with HA

compound	ν_{Fe-H}/cm^{-1}	δ_H (J_{HP}/Hz)	δ_P
Cp*(dppe)FeH	1844 (s)	−17.32 (67)	107.97
Cp*(dppe)FeH···HA[a]	1830 (sh)	*b*	*b*
$[Cp^*(dppe)Fe(H_2)]^+$	*c*	−12.50 (broad)	93.39
$[Cp^*(dppe)Fe(H)_2]^+$	1940 (w)	−7.98 (73)	90.97

[a] Observed for HA = TFE. [b] Not significantly shifted from the values of free Cp*Fe(dppe)H (see text). [c] Not observable (see text).

Results and Discussion

(a) Interaction with HBF_4. Spectral Characteristics of the Classical and Nonclassical Protonation Products. Half-sandwich Fe hydride complexes are relatively rare.[8,9,32−37] Those containing two or more hydride ligands display a preference for the classical Fe(IV) isomer, the Fe(II) dihydrogen isomer being observable only for less donating ligand environments. For the Cp*-dppe derivative, both the dihydrogen complex, $[Cp^*Fe(dppe)(H_2)]^+$, and the classical dihydride complex, $[Cp^*Fe(dppe)(H)_2]^+$, have been described as the kinetic and thermodynamic protonation products, respectively, resulting from the treatment of the hydride complex with HBF_4.[8,9] The faster formation of the dihydrogen complex relative to the dihydride tautomer illustrates that proton transfer to the hydride site is more facile than that to the metal center, as is also well established for a number of other complexes.[3,6,7]

Because the spectral characterization of the two tautomeric dihydride cations in solution was previously restricted to NMR, we have reinvestigated the HBF_4 protonation by IR and UV−visible techniques, in addition to NMR. A careful reinvestigation of the longitudinal relaxation time as a function of temperature for the starting hydride and protonation products, however, provides useful new information. The ^{1}H (hydride resonance) and ^{31}P NMR chemical shifts for the three species involved are summarized in Table 1.[8,9] The proton transfer is immediate and quantitative at 200 K in CD_2Cl_2, as is shown by the NMR monitoring, yielding the dihydrogen complex selectively. Subsequent slow warming confirmed the previously reported

(30) Roger, C.; Hamon, P.; Toupet, L.; Rabaâ, H.; Saillard, J.-Y.; Hamon, J.-R.; Lapinte, C. *Organometallics* **1991**, *10*, 1045−1054.
(31) Binstead, R. A.; Jung, B.; Zuberbühler, A. D. *Specfit/32*; 2000 Spectrum Software Associates: Chapel Hill, NC, 2000.
(32) Jetz, W.; Graham, W. A. G. *Inorg. Chem.* **1971**, *10*, 1159−1165.
(33) Paciello, R. A.; Manriquez, J. M.; Bercaw, J. E. *Organometallics* **1990**, *9*, 260−165.
(34) Hamon, P.; Hamon, J.-R.; Lapinte, C. *J. Chem. Soc., Chem. Commun.* **1992**, 1602−1603.
(35) Jiménez-Tenorio, M.; Puerta, M. C.; Valerga, P. *Organometallics* **1994**, *13*, 3330−3337.
(36) Tilset, M.; Fjeldahl, I.; Hamon, J. R.; Hamon, P.; Toupet, L.; Saillard, J. Y.; Costuas, K.; Haynes, A. *J. Am. Chem. Soc.* **2001**, *123*, 9984−10000.
(37) Jia, G.; Ng, W. S.; Yao, J.; Lau, C.-P.; Chen, Y. *Organometallics* **1996**, *15*, 5039−5045.

Table 2. Longitudinal Relaxation Times at 400 MHz in CD_2Cl_2 for Cp*Fe(dppe)H and for the Products Deriving from Its Interaction with TFE (TFE/Fe = 3)

	T_1/ms		
T/K	FeH	FeH + TFE	$Fe(H_2)^+$
190		25	24
200		12	15
220	349.7	3.9	11
225	328.2		
230	311.4		9.6
235	280		
240	241.4	0.67	10.2
245	223.4		
250	200		
255	182.8		
260	173		

conversion to the classical dihydride complex at temperatures above 250 K. The classical dihydride product is stable in CD_2Cl_2 at room temperature for a few minutes. Longer monitoring (few hours) revealed, however, a previously undetected further evolution with formation of a paramagnetic product, which is shown to correspond to the previously described complex $[Cp^*Fe(dppe)Cl]^+$.[30] No equivalent decomposition occurs in THF. This decomposition did not prevent us from studying the details of the proton-transfer process in CH_2Cl_2, which occurs on a much faster time scale.

The relaxation times as a function of temperature are shown in Table 2. It can be noted that complex Cp*Fe(dppe)H does not show a T_1 minimum. Rather, T_1 keeps decreasing as the temperature increases. Fitting the T_1 data for the dihydrogen complex $[Cp^*Fe(dppe)(H_2)]^+$, on the other hand, gives a T_{1min} time of 9.7 ms at 230 K, in good agreement with the minimum of 7 ms obtained by Hamon et al. at 223 K and 300 MHz.[9] This behavior is not expected because the two complexes have practically the same inertia moment and should therefore exhibit a T_{1min} at approximately the same temperature when working at the same field strength. This discrepancy can only be rationalized by the presence of small amounts of the paramagnetic complex $[Cp^*Fe(dppe)H]^+$ in the neutral precursor. This complex has been shown to be stable, even at room temperature,[8] which is a relatively rare occurrence for paramagnetic hydrides.[38] The two complexes must be involved in a degenerate exchange with a rate that increases with temperature, and additional observations made in the presence of fluorinated alcohols (vide infra) confirm this view. It is clear that the concentration of the cationic paramagnetic complex is very small and therefore does not affect the resonance line width, whereas it affects the relaxation times. Its presence does not affect, on the other hand, the T_1 time of the dihydrogen complex, $[Cp^*Fe(dppe)(H_2)]^+$, because a hypothetical exchange between these two complexes would be much slower than the degenerate exchange with Cp*Fe(dppe)H.

In a subsequent experiment carried out in CH_2Cl_2, IR monitoring in the Fe−H stretching region provided the spectral changes shown in the upper part of Figure 1. The starting hydride complex is characterized by a relatively strong ν(MH) band at 1844 cm^{-1} (ϵ = 8.81 and 6.32 L mol^{-1} cm^{-1} at 200 and 290 K, respectively) in CH_2Cl_2 solution, which is displaced relative to the solid state (1869 cm^{-1}),[8] plus a few weaker

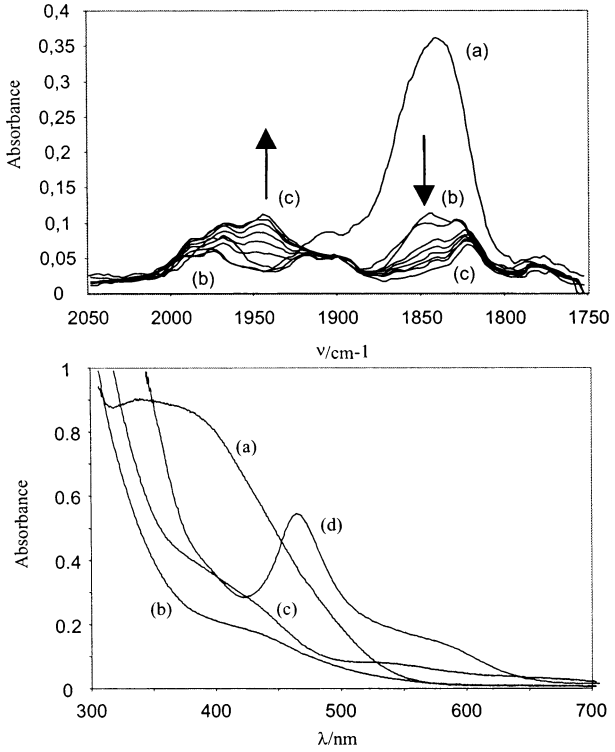

Figure 1. Spectral changes (IR, above; UV−visible, below) observed for the protonation of Cp*Fe(dppe)H by HBF_4 in CH_2Cl_2. (a) Before addition of HBF_4 (T = 200 K); (b) after addition of HBF_4 (T = 200 K); (c) T = 290 K (after a few minutes); (d) T = 290 K, after several hours. [Fe] = 0.03 M (IR); 0.01 M (UV−visible); HBF_4/Fe = 1.

features in the 2000−1750 cm^{-1} region which correspond to overtones of aryl group vibrations, see spectrum a. The HBF_4 addition at 200 K causes the essentially complete disappearance of this band, see spectrum b. Unfortunately, the IR spectra (measured in 3000−1500 cm^{-1} region) do not reveal any absorbance for ν(H−H) and $\nu(MH_2)$ vibration modes. These bands are known to be very weak and often hidden under strong CH vibrations or overtones.[39] This spectrum remains essentially unchanged upon raising the temperature, until it reaches ca. 250 K. At higher temperatures, conversion to the classical dihydride complex occurs, yielding eventually spectrum c. A weak band at 1940 cm^{-1} can clearly be attributed to the cationic dihydride complex, while the higher frequency shoulders of this band are probably overtones of the aryl group vibrations. Such a significant high-frequency shift ($\Delta\nu_{MH}$ = +100 cm^{-1}) of the ν(MH) band is typical for transition metal protonation yielding a cationic classical product.[20,40,41]

Yet another experiment was carried out with UV−visible monitoring. The resulting spectral changes are shown in the lower part of Figure 1. The starting hydride complex has a relatively strong and broad metal−ligand charge-transfer band[42] with a maximum around 388 nm (ϵ = 2370 L mol^{-1} cm^{-1}), spectrum a. The dihydrogen complex, spectrum b, has a much weaker and featureless absorption (ϵ = 640 L mol^{-1} cm^{-1} at 388 nm). Evolution to the classical dihydride complex is accompanied by a minor change of the spectrum, which is more

(38) Poli, R. In *Recent Advances in Hydride Chemistry*; Poli, R., Peruzzini, M., Eds.; Elsevier Science: Amsterdam, 2001; pp 139−188.

(39) Bender, B. R.; Kubas, G. J.; Jones, L. H.; Swanson, B. I.; Eckert, J.; Capps, K. B.; Hoff, C. D. *J. Am. Chem. Soc.* **1997**, *119*, 9179−9190.
(40) Girling, R. B.; Grebenik, P.; Perutz, R. N. *Inorg. Chem.* **1986**, *25*, 31−36.
(41) Abdur-Rashid, K.; Fong, T. P.; Greaves, B.; Gusev, D. G.; Hinman, J. G.; Landau, S. E.; Lough, A. J.; Morris, R. H. *J. Am. Chem. Soc.* **2000**, *122*, 9155−9171.

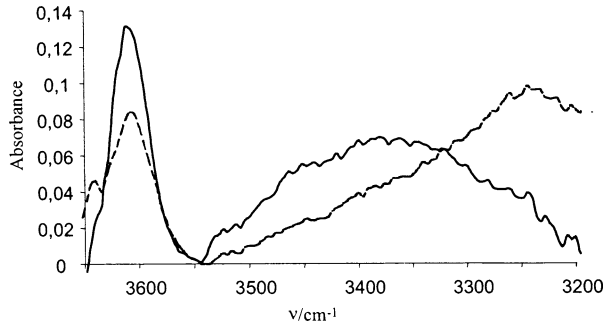

Figure 2. IR spectra in the $\nu(R_FO-H)$ stretching region showing the interaction between Cp*Fe(dppe)H and MFE or TFE in CH_2Cl_2. Solid line: [Fe] = 0.15 M; [MFE] = 0.015 M. Dashed line: [Fe] = 0.13 M; [TFE] = 0.01 M.

Table 3. Parameters of the Dihydrogen-Bonding Interaction between Cp*Fe(dppe)H and MFE or TFE in CH_2Cl_2

ROH	P_i	$\nu_{OH(free)}$ cm^{-1}	$\nu_{OH(bonded)}$ cm^{-1}	$\Delta\nu$ cm^{-1}	$\Delta H°$ [a] kcal mol^{-1}	E_j [b]
MFE	0.74	3608	3362	246	−4.6	1.35
TFE	0.89	3594	3240	354	−5.9	1.38

[a] $\Delta H°$ parameter calculated by eq 1, mean error ±0.4 kcal mol^{-1}. [b] E_j parameter calculated by eq 2, $\Delta H_{11}° = -4.6$ kcal mol^{-1} for CH_2Cl_2.[16]

accurately determined by the analysis of the stopped-flow kinetic data (vide infra). The dihydride spectrum is given by trace c (ϵ = 1093 L mol^{-1} cm^{-1} at 388 nm). However, the UV−visible monitoring shows that this product is unstable in dichloromethane at room temperature and decomposes over several hours to afford trace d, which is characterized by a weak d−d transition with maximum at 466 nm (ϵ = 587 L mol^{-1} cm^{-1}).[42] No analogous evolution occurs in THF. This behavior is fully consistent with the results of the NMR investigation described above. The spectral characteristics of the nonclassical and classical hydrides and for the final $[Cp^*Fe(dppe)Cl]^+$ decomposition product now allow us to study the mechanism of the protonation process in more detail.

(b) Interaction with MFE and TFE. Determination of Hydrogen-Bonding Enthalpy and Basicity Factor E_j of the Proton Accepting Site. The interaction of MFE and TFE (on a short time scale, vide infra) with excess Cp*Fe(dppe)H leads to hydrogen-bond formation without any complication from proton-transfer processes.[43] This interaction could conveniently be investigated according to well-established protocols.[11] The spectral features in the $\nu(R_FO-H)$ stretching region (Figure 2) show the expected stronger interaction with the more fluorinated alcohol, as indicated by the greater $\Delta\nu$ ($\nu_{OH(free)}-\nu_{OH(bonded)}$). The resulting interaction enthalpies were obtained by Iogansen's empirical correlation (eq 1)[44] and are reported in Table 3. They show that the hydrogen bonds between complex Cp*Fe(dppe)H and MFE or TFE have medium strength (4−6 kcal/mol). The enthalpy for the interaction with TFE was also determined by van't Hoff's method, which required investigations at variable temperature and furnishes also the interaction entropy. The equilibrium shifts toward the hydrogen-bonded adduct upon cooling from 290 to 250 K, see Figure 3, yielding $\Delta H° = -5.4 \pm 0.3$ kcal mol^{-1} and $\Delta S° = -13.6 \pm 0.9$ cal mol^{-1} K^{-1}. The

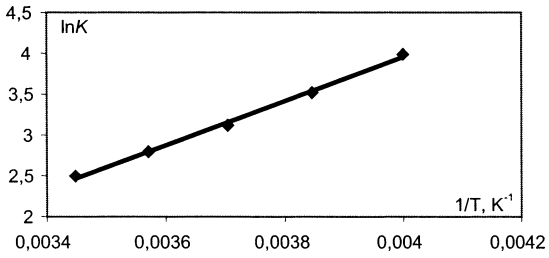

Figure 3. Temperature dependence of ln K for the interaction between Cp*Fe(dppe)H and TFE in CH_2Cl_2. [Fe] = 0.13 M; [TFE] = 0.01 M.

enthalpy values obtained by the two different methods agree rather well with each other, confirming once again the applicability of the correlation given by eq 1. The equilibrium constant for the hydrogen-bond formation is K = 10 (298 K) and 870 (200 K). It can reasonably be predicted that the more acidic alcohols HFIP and PFTB provide higher equilibrium constants for hydrogen-bond formation, leading to the prediction that most of the hydride complex is in the hydrogen-bonded form in the presence of excess alcohol, especially at low temperatures.

$$-\Delta H° = \frac{18\Delta\nu}{\Delta\nu + 720} \quad (1)$$

Use of the empirical relationship in eq 2[45] led to the calculation of the E_j basicity factors, see Table 3. As expected, the values obtained for E_j by use of the two different alcohols are essentially identical. This places the Cp*Fe(dppe)H complex among the most basic hydrides so far investigated, for example, $[ReH_3(\eta^4\text{-}N(CH_2CH_2PPh_2)_3)]$ (E_j = 1.45)[21] and $\{(MeC(CH_2PPh_2)_3\}Ru(CO)H_2$ (E_j = 1.39).[46] Note, however, that hydrogen bonding is established with the metal atom in the first case and with the hydride ligand in the second case. Therefore, our next step was the establishment of the hydrogen-bonding site for the title Fe hydride complex.

$$E_j = \frac{\Delta H°}{\Delta H_{11}° P_i} \quad (2)$$

(c) Establishment of the Hydrogen-Bonding Site. It is now well established that hydrogen bonding to a hydride ligand site, also termed "nonclassical or dihydrogen bonding", causes a low-frequency shift of the M−H band,[11] whereas the involvement of the metal lone pair(s) as proton acceptor(s) for hydrogen bonds shifts other M−X stretching vibrations (notably the M−H band) to a higher frequency range.[12,20,21] Therefore, we have studied the interaction between the hydride complex and different proton donors by IR spectroscopy in the ν(MH) region. The alcohol addition was first carried out and studied at low temperatures. All alcohols induce the development of a low-frequency shift of the ν(MH) band (1836−1828 cm^{-1}), which indicates the formation of the dihydrogen-bonded complex $Cp^*(dppe)FeH\cdots HOR_F$. The extrapolation of the variable-temperature data for hydrogen bonding with TFE (Figure 3) gives a formation constant of 870 at 200 K. Thus, essentially all of the hydride complex is in the hydrogen-bonded state under these conditions. Consequently, the ν(MH) band at 1830 cm^{-1}

(42) Lever, A. B. P. *Inorganic Electronic Spectroscopy*, 2nd ed.; Elsevier: Amsterdam, 1984.
(43) An NMR investigation also confirmed the absence of any proton transfer at room temperature in the presence of 12 equiv of MFE.
(44) Iogansen, A. V. *Hydrogen Bond*; Nauka: Moscow, 1981; p 134.
(45) Iogansen, A. V. *Theor. Exp. Khim.* **1971**, *7*, 312−317.
(46) Bakhmutov, V. I.; Bakhmutova, E. V.; Belkova, N. V.; Bianchini, C.; Epstein, L. M.; Masi, D.; Peruzzini, M.; Shubina, E. S.; Vorontsov, E. V.; Zanobini, F. *Can. J. Chem.* **2001**, *79*, 479−489.

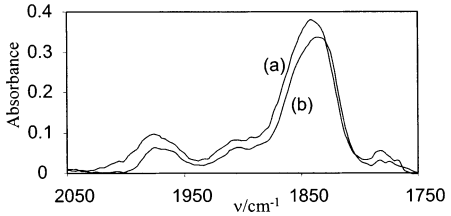

Figure 4. IR study of the interaction between Cp*Fe(dppe)H (0.038 M) and TFE in CH_2Cl_2 at 200 K. (a) Without TFE. (b) With TFE (3 equiv).

in Figure 4 (trace b) can be unambiguously attributed to the Fe−H stretching vibration in the dihydrogen-bonded complex. The absence of a high-frequency shoulder shows that no significant amount of hydrogen bond at the metal center, that is, Cp*(dppe)HFe···HOR_F, is present, see Figure 4.[47]

In conclusion, the IR study shows the establishment of hydrogen bonding involving the hydride ligand as the first step of the proton transfer leading to the dihydrogen complex. In comparison with previous literature data,[12] the rather high E_j value suggests that this hydride can be protonated by fluorinated alcohols such as HFIP and PFTB in CH_2Cl_2. Indeed, the ν(MH) band intensities observed in the presence of these alcohols dramatically decrease with a temperature decrease, especially when PFTB is used. This contrasts with the intensity increase in the absence of alcohol, see section a. This change is reversible in the low-temperature range and signals a reversible proton-transfer process leading to the dihydrogen complex.

(d) Interaction with PFTB, HFIP, and TFE: NMR Investigations. ^{1}H NMR investigations of CD_2Cl_2 solutions containing Cp*Fe(dppe)H and the three fluorinated alcohols provided only qualitative information on the nature of the species involved and on the chemical equilibria. In all cases, the alcohol addition to the hydride solution at low temperature yielded two hydride resonances, a broadened triplet at δ ca. −17.3 and a broad resonance at δ ca. −12.5. These chemical shifts are essentially identical to those of free Cp*Fe(dppe)H and Cp*Fe(dppe)$(H_2)^+BF_4^-$, respectively, and are not significantly affected by the temperature, alcohol nature, and alcohol/Fe ratio. The dihydrogen complex, Cp*Fe(dppe)$(H_2)^+$, is probably present in solution as a free ion, **III**, rather than hydrogen bonded to the alkoxide ion, **II** (Scheme 1), as will be further argued later. The −17.3 resonance is attributed to the rapidly exchanging equilibrium mixture of Cp*Fe(dppe)H and Cp*(dppe)FeH···PFTB (whose presence is proven by the IR study, vide supra). The ^{31}P{^{1}H} spectrum correspondingly gives two signals at δ ca. 93.8 and at δ ca. 108. These are also essentially unshifted with respect to the resonances of Cp*Fe(dppe)$(H_2)^+BF_4^-$ and free Cp*Fe(dppe)H, respectively.

The nature of the alcohol and the alcohol/Fe ratio strongly affect the proton-transfer equilibrium position with the nonclassical intermediate and the temperature at which further evolution to the classical product starts to occur (ca. 250 K for PFTB, 270 K for HFIP, and room temperature for TFE). There was no evidence for the formation of products other than the classical dihydride complex on a short time scale (few minutes) at room temperature. In particular, there were no resonances that could be assigned to a hypothetical Cp*Fe(dppe)(OR_F) product, which may result from dihydrogen evolution. However, a longer NMR monitoring revealed the slow formation (few hours at room temperature) of the same paramagnetic product, [Cp*Fe(dppe)Cl]$^+$, which is observed by using HBF_4.

The initial proton transfer to yield the intermediate dihydrogen complex is more shifted toward the right, at constant alcohol/Fe ratio, as the alcohol acidity increases (TFE < HFIP < PFTB) and, for the same alcohol, as the alcohol/Fe ratio increases. For instance, the FeH/Fe$(H_2)^+$ ratio is approximately 45:55 when using PFTB/Fe = 1, 75:25 when using HFIP/Fe = 3, and 40:60 at TFE/Fe = 10 (220 K).

The starting hydride resonance (mixture of starting hydride in fast equilibrium with the hydrogen-bonded adducts) broadens significantly as the temperature increases (see Table 4), whereas the resonance of the dihydrogen complex maintains approximately the same width (ca. 25 Hz) independent of the temperature, nature of the alcohol, and alcohol/Fe ratio. This phenomenon cannot result from a rapid exchange between the free and hydrogen-bonded hydride complexes, nor from an exchange between the hydrogen-bonded complex and the proton-transfer product. In the first case, the peak should sharpen upon increasing the temperature because coalescence is already achieved, whereas in the second case the broadening phenomenon should be equally observable on both resonances, contrary to the observation. The most likely explanation for the observed phenomenon is the self-exchange process with trace amounts of the one-electron oxidation product, the paramagnetic [Cp*Fe(dppe)H]$^+$ ion, whose presence is also responsible for the unusual temperature dependence of the T_1 time for the starting hydride complex (vide supra). Further indication that this is the correct explanation is the measurement of unrealistically small relaxation times (T_1) for the broad hydride resonance in the presence of TFE (see Table 2). The longitudinal relaxation time has been frequently used as a criterion for establishing the presence of dihydrogen-bonding interactions. The T_1 value slightly decreases relative to that of the starting hydride complex, because of the additional dipolar relaxation induced by the hydrogen-bonded proton. The presence of dihydrogen bonding for the Cp*Fe(dppe)H complex, however, could not possibly give such low values for T_1 (e.g., 0.67 ms at 240 K, see Table 2), even lower than for the dihydrogen complex product where the H−H distance is certainly shorter. This value can only result from the fast relaxation induced by the unpaired electron in the oxidized 17-electron complex, with which the starting hydride complex is in fast degenerate exchange. Shaking the NMR solutions with Zn/Cu alloy inside the NMR tube did not,

Table 4. Band Widths at Half Height for [Cp*Fe(dppe)(H_2)]$^+$ and Hydrogen-Bonded Cp*Fe(dppe)H Adducts in CD_2Cl_2 as a Function of Temperature[a]

	$w_{1/2}$/Hz		
T/K	FeH···TFE	FeH···HFIP	FeH···PFTB
180		65	triplet
200	190	142	170
220	270	230	230
230	350	320	290
240	510	480	440
250	760		
260		1100	1280

[a] C_{FeH}° = 0.05−0.07 M. Identical values were observed for different alcohol/Fe ratios.

(47) The occasional observation of a high-frequency shoulder is attributed to variable amounts of the 17-electron complex [Cp*Fe(dppe)H]$^+$,[8] resulting from adventitious oxidation of the extremely air-sensitive hydride complex. Indeed, a synthesized sample of this complex yields an Fe−H stretching vibration at 1868 cm^{-1} in CH_2Cl_2.

unfortunately, eliminate this problem. This occurrence unfortunately renders a more thorough NMR characterization of hydrogen bonding for the Cp*Fe(dppe)H hydride complex impossible.

The reason the starting hydride band is broader and T_1 is shorter in the presence of alcohol may be the result of the partial conversion to the protonation product, increasing the [Cp*Fe(dppe)H]$^+$/Cp*Fe(dppe)H ratio. Additional oxidation upon introduction of the alcohol cannot be excluded. In any event, the extent of this oxidation process remains small. If a significant amount of hydride complex had been oxidized, the resonance would not only broaden but also shift to an extent that would depend on temperature. In fact, this is not the case, the chemical shift being essentially temperature independent as in the alcohol-free solution.

(e) Interaction with PFTB, HFIP, and TFE: IR Investigations. Low-temperature IR spectroscopic studies also provide qualitative indications on the interaction between Cp*Fe(dppe)H and fluorinated alcohols, leading to proton transfer. The essential findings from the NMR study were confirmed by the IR investigation: (i) the proton-transfer equilibrium between the hydrogen-bonded system and the dihydrogen complex is shifted toward the protonation product to a greater extent for stronger alcohols and for higher alcohol/Fe ratios; (ii) conversion of the overall mixture to the final classical dihydride product started to occur at a higher temperature for the weaker alcohols.

With PFTB, the complete disappearance of the starting material occurs when using a 3-fold excess at 200 K in CH_2Cl_2, whereas an equilibrium situation is obtained when the alcohol is used stoichiometrically. As in the NMR experiment, the isomerization started to occur upon raising the temperature above 250 K. For the HFIP experiment, larger excess amounts of alcohol are required to consume a substantial amount of the hydride precursor at low temperature. For TFE, only ca. 50% of dihydrogen complex was formed when using a 15-fold excess of TFE at 200 K (cf., 98% for HFIP under otherwise identical conditions). In addition, the proton transfer is much slower (>30 min for TFE vs <5 min for HFIP at 200 K). No quantitative kinetics information, however, can be obtained using this technique. In all three cases, the reversibility of the IR spectral changes with temperature (below the temperature at which isomerization to the final classical dihydride product starts to occur) qualitatively indicates that the proton-transfer equilibrium shifts toward the dihydrogen complex when temperature decreases, but no quantitative thermodynamic information can be derived.

(f) Interaction with PFTB, HFIP, and TFE: Preliminary UV−Visible Investigations. Finally, the Cp*Fe(dppe)H−HA interaction was investigated by UV−visible spectroscopy in CH_2Cl_2, because this technique is more adept to yielding quantitative results. The study confirmed the two-step pathway already established by the IR and NMR techniques, followed by the slow decomposition to the paramagnetic [Cp*Fe(dppe)Cl]$^+$. The evolution of the UV−visible spectrum is qualitatively identical with respect to the corresponding protonation by HBF_4 (see Figure 1, bottom part). This evolution appeared best suited to detailed kinetic investigations of the proton-transfer process, which will be described below in section g.

The interaction of Cp*Fe(dppe)H with PFTB (1:5 ratio) at 200 K immediately gives the dihydrogen complex quantitatively,

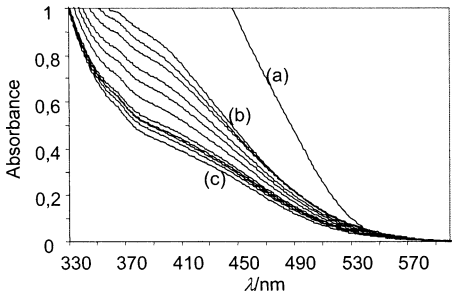

Figure 5. UV−visible study of the interaction between Cp*Fe(dppe)H and HFIP (5 equiv) in CH_2Cl_2. [Fe] = 0.02 M. (a) Before the HFIP addition. (b) T = 270 K. (c) T = 200 K. The other intermediate spectra correspond to 265−225 K (5 K steps).

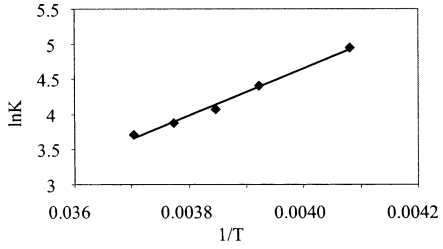

Figure 6. Temperature dependence of ln K for the interaction between Cp*Fe(dppe)H and HFIP in CH_2Cl_2.

followed by transformation to the dihydride isomer at temperatures greater than 250 K and finally to [Cp*Fe(dppe)Cl]$^+$ over several hours at room temperature. With HFIP, the proton-transfer equilibrium could be investigated in a wider temperature range and for several HFIP/Fe ratios. In the 200−270 K temperature range, the UV−visible spectral changes are perfectly reversible and indicate, in agreement with the IR evidence, a temperature dependence of this equilibrium, see Figure 5. The UV−visible properties of the dihydrogen-bonded complexes are essentially indistinguishable from those of the free hydride complex, as confirmed by the fast kinetics studies, vide infra. This is reasonable, because the hydrogen-bonding interactions should perturb the electronic structure of the metal center only in a minimal way. The least absorbing species in this equilibrium solution, however, is the dihydrogen complex, see Figure 1. Therefore, the overall changes shown by Figure 5 are consistent with the presence of a greater relative amount of the dihydrogen complex at lower temperatures.

The reversibility of this process enabled us to obtain the equilibrium constant for eq 3 assuming that all hydride is in the dihydrogen-bonded form at 200−270 K (vide supra, section b) and that the equilibrium involves a second alcohol molecule (vide infra, section g). The van't Hoff plot (Figure 6) gives the enthalpy ($\Delta H^\circ = -6.6 \pm 0.9$ kcal mol^{-1}) and the entropy ($\Delta S^\circ = -17.2 \pm 1.4$ eu) of the process shown in eq 3.

$$\text{Cp*Fe(dppe)H}\cdots\text{HA} + \text{HA} \rightleftarrows [\text{Cp*Fe(dppe)(H}_2)]^+[\text{AHA}]^- \quad (3)$$

For TFE, the slow equilibration rates made it impractical to determine the accurate equilibrium position at low temperatures. In addition, the smaller proton-transfer equilibrium constant required the use of greater alcohol concentrations, with consequent crystallization of the excess alcohol at low temperatures in dichloromethane.

Scheme 2

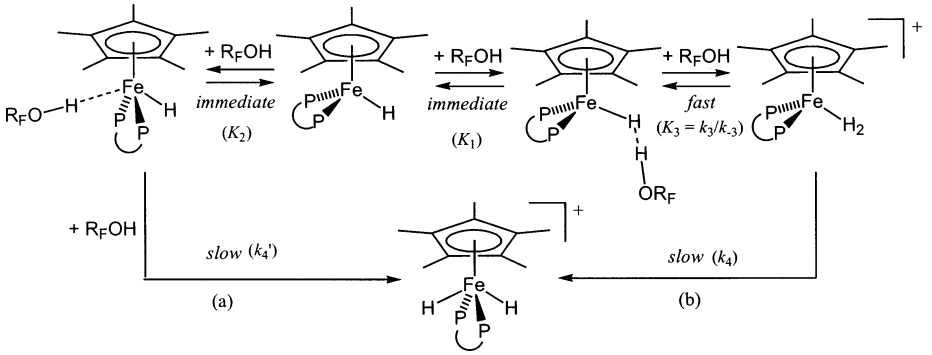

Scheme 3

$$\mathbf{Fe} \underset{k_{-3obs}}{\overset{k_{3obs}}{\rightleftharpoons}} Fe(H_2)^+$$

$$([\mathbf{Fe}] = [FeH] + [FeH\cdots HA] + [HFe\cdots HA])$$

$$Fe(H_2)^+ \xrightarrow{k_{4obs}} Fe(H)_2^+$$

$$Fe(H)_2^+ \xrightarrow{k_{5obs}} FeCl^+$$

(g) Kinetics Investigations of the Proton Transfer from TFE, HFIP, PFTB, and TFA. The collective spectroscopic studies of the hydride−HA interactions described in the previous section suggest Scheme 2, in line with previous knowledge in this field as outlined in the Introduction. In principle, each different hydrogen-bonded complex can be seen as an intermediate leading to a different proton-transfer product. The dihydrogen bond (K_1) would lead to the nonclassical product ($K_3 = k_3/k_{-3}$), while the hydrogen bond to the metal center (K_2) would lead to the classical product (k_4'). However, the classical dihydride complex may also be obtained directly from the nonclassical tautomer (k_4). The second hypothesis appears consistent with the observation by Hamon et al. that the isomerization also takes place for the isolated dihydrogen complex in the solid state.[9] The results of a more detailed kinetic investigation by UV−visible monitoring allow us to throw more light on this dichotomy.

The reactions with the three fluorinated alcohols TFE, HFIP, and PFTB were carried out in CH_2Cl_2 at 298 K under pseudo-first-order conditions with HA/Fe ratios in the 30−200 range. The entire kinetics investigation required the use of both stopped-flow and classical mixing and monitoring methods. In all cases, the spectrum recorded immediately after mixing (ca. 1 ms) is indistinguishable from that of the pure hydride in the absence of alcohol,[48] proving that the hydrogen bonding does not significantly perturb the electronic structure of the metal center. The establishment of hydrogen bonds is a diffusion-controlled step.[49] The investigations yielded the rate constants for three separate processes, as indicated in Scheme 3 [Fe = Cp*Fe(dppe)]. Although the initial equilibrium may include, in principle, the hydrogen-bonded adducts involving the hydride site and those at the metal site, [FeH···HA] and [HFe···HA], the latter species was not found in the present case.

For the PFTB process, the first measurable step was complete within a fraction of a second and could be accurately measured only by stopped-flow kinetics. The second, slower step was also accessible from the stopped-flow data. The two processes occur on quite different time scales, and the first process is essentially quantitative even for the lowest [HA]/[FeH] ratio, rendering the kinetic analysis straightforward. These two processes correspond to the proton-transfer equilibrium yielding the dihydrogen intermediate and to the isomerization process, respectively. This is confirmed by comparison of the extrapolated spectra of intermediate and product (as obtained from a global Specfit analysis) with those obtained from the HBF_4 protonation (see Figure 1). The first-order dependence of the proton-transfer rate constant (k_{3obs}) on the alcohol concentration is shown in Figure 7a. The intercept is zero within experimental error (0.1 ± 0.7 s^{-1}), confirming the assumption of irreversibility for this step. The subsequent rate constants, k_{4obs} and k_{5obs}, on the other hand, do not show any dependence on the alcohol concentration. All rate constants are collected in Table 5.

For the HFIP run, the first step required a few seconds and partially overlapped with the second kinetics. In addition, the above determined thermodynamic data for this proton-transfer step (extrapolated equilibrium constant of 7.97 at 298 K) suggest that this may be equilibrated, even for the relatively high HFIP/Fe ratios employed in this kinetic study. However, a good fit was possible for the model A → B → C, yielding individual observed rate constants for each step. The first step (proton transfer) has a first-order dependence on HFIP, and the intercept is close to the experimental error ($k_{-3obs} = 0.21 \pm 0.13$ s^{-1}), see Figure 7b. Thus, this step is almost irreversible under the experimental conditions used for this kinetic experiment. Even though it is affected by a large uncertainty, the estimated k_{3obs}/k_{-3obs} ratio is consistent with the estimated proton-transfer equilibrium constant from the van't Hoff analysis (vide supra). The values of k_{4obs} and k_{5obs} are independent from the alcohol concentration. Furthermore, and most notably, they are also independent of the alcohol nature, the values obtained for PFTB and HFIP being very close to each other, see Table 5.

Contrary to the PFTB and HFIP reactions, the proton transfer from TFE led to a single measurable kinetics for the transformation of FeH to the classical dihydride product. The reason for this result is that the second step is faster than the first one. This was too slow for the stopped-flow time scale, but it could be accessed by regular mixing and monitoring in an airtight cuvette. A complication in this case was the contamination by the final transformation to the paramagnetic chloro complex. However, the SPECFIT global analysis afforded reasonably

(48) Comparative shootings of the hydride solution against the alcohol and against neat CH_2Cl_2 show an identical first spectrum (ca. 1 ms).
(49) Scheiner, S. *Hydrogen bonding: A Theoretical Perspective*; Oxford University Press: New York, 1997.

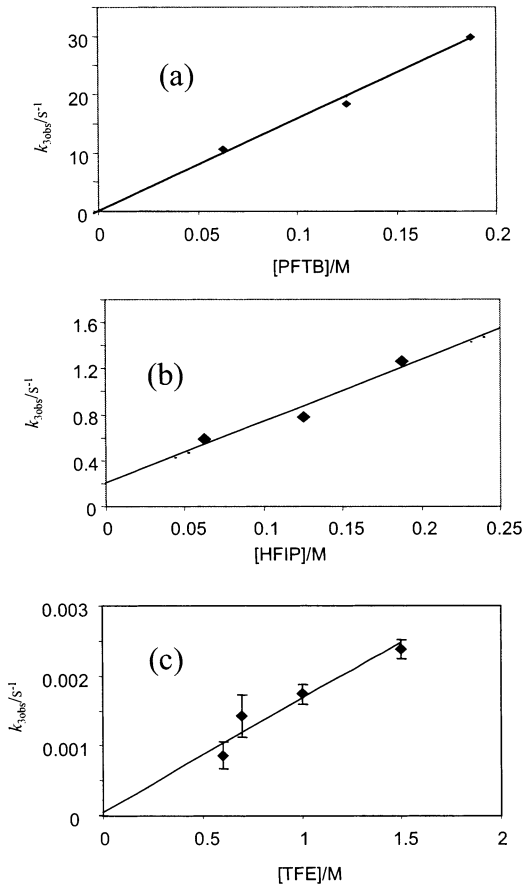

Figure 7. Pseudo-first-order rate constants for the first step of the proton transfer from HA to Cp*Fe(dppe)H [k_{3obs}; HA = PFTB (a), HFIP (b), TFE (c)].

Table 5. Observed Rate Constants for the Reaction between Cp*Fe(dppe)H and HA[a]

HA	$k_{3obs}[HA]^{-1}/s^{-1}\,M^{-1}$	k_{4obs}/s^{-1}	k_{5obs}/s^{-1}
TFA	*b*	$(6.4 \pm 0.2) \times 10^{-2}$	
PFTB	156 ± 5	$(7.6 \pm 0.2) \times 10^{-2}$	$(2.3 \pm 0.3) \times 10^{-4}$
HFIP	5.4 ± 0.9	$(6.8 \pm 0.2) \times 10^{-2}$	$(2.1 \pm 0.3) \times 10^{-4}$
TFE	$(1.5 \pm 0.3) \times 10^{-3}$	*c*	$(2.2 \pm 0.6) \times 10^{-4}$

[a] See Scheme 3. [b] Too fast to be measured by stopped-flow methods. [c] Not measurable because faster than k_{3obs}.

precise values for both k_{3obs} and k_{5obs}. The value of k_{3obs} was linearly dependent on the alcohol concentration, with a zero intercept within experimental error as for the previous cases, $(1.6 \pm 3) \times 10^{-4}$ s^{-1}. The value of k_{5obs} does not show any significant dependence on the alcohol concentration and is very close to those observed with the other alcohols (see Table 5).

To further widen the acidity range of the proton donor, we also carried out a kinetic study of the protonation with trifluoroacetic acid (TFA). With this acid, the first step was too fast to measure by the stopped-flow technique, the first recorded spectrum after ca. 1 ms corresponding already to that of the intermediate dihydrogen complex (i.e., spectrum b in Figure 1). Further transformation to the classical tautomer (spectrum c in Figure 1) followed clean first-order kinetics, the k_{4obs} being once again independent of the acid concentration and close in value to those observed for the fluorinated alcohols (see Table 5).

In summary, proton donors instantaneously establish hydrogen bonding at the hydride site. This is in agreement with the general knowledge that they are diffusion-controlled, barrierless reactions.[49] The subsequent step is proton transfer to the hydride site, whose rate and equilibrium constant increase in the order TFE < HFIP < PFTB < TFA, as the acidity of the proton donor increases. This rate has a first-order dependence on the alcohol concentration (established experimentally for the three alcohols).

If one neglects the establishment of the hydrogen bonds, the first-order dependence on the alcohol concentration would point to a rather simple bimolecular elementary process, whereby one alcohol molecule transfers its proton to the hydride complex in a direct, single-step process. This would also explain the rate constant dependence on the proton donor acidity. However, the measured thermodynamic parameters for hydrogen bonding with TFE (Figure 3) allow us to estimate a 6:1 FeH···HX/FeH ratio under the conditions used for the stopped-flow kinetics study. When HFIP and PFTB are used, the constant for dihydrogen-bond formation will be even higher. Therefore, the [FeH···HA] complex predominates in the mixture which transforms further into nonclassical protonation product.

The starting point for the first kinetics process is not the pure hydride precursor but rather the equilibrium mixture with the hydrogen-bonded adducts, Scheme 3. A straightforward manipulation of the rate expression leads to eq 4, which can be simplified as shown at high alcohol concentrations (quantitative formation of the hydrogen-bonded adducts). Therefore, the observed first-order dependence on HA implies the intervention of a second molecule in the rate-determining step, as indicated in Scheme 4. If a second alcohol molecule were not involved in the proton-transfer step, the k_{3obs} expression would lead to an essentially alcohol-independent observed rate constant. This observation suggests that a direct proton transfer leading to a salt which contains a free alkoxide anion does not occur. The involvement of a second alcohol molecule presumably renders the proton-transfer process thermodynamically more favorable and faster via the establishment of a hydrogen-bonding interaction and the formation of an alcohol/alkoxide homoconjugate pair (see Scheme 4). This homoconjugate pair formation has been noted in other proton-transfer processes to hydride complexes[3,50] and is comforted by theoretical calculations.[51] Because of this homoconjugate pair formation, we consider it unlikely that the alkoxide ion also remains hydrogen bonded to the dihydrogen ligand in the dichloromethane solvent used. The product, therefore, is probably present in solution in the form of free ions.

$$k_{3obs} = \frac{k_3 K_1 [HA]^2}{1 + (K_1 + K_2)[HA]} \approx \frac{k_3 K_1}{K_1 + K_2}[HA]$$

The question remains as to the intimate mechanism of the tautomerization process, as indicated by the two possible pathways a and b in Scheme 2. Both pathways would lead to a zero-order dependence on the proton donor concentration (see Supporting Information), as was experimentally observed. Therefore, they cannot be distinguished on this basis. However, the independence of the rate constant on the nature of the proton donor strongly points toward an internal reorganization mech-

(50) Belkova, N. V.; Ionidis, A. V.; Epstein, L. M.; Shubina, E. S.; Gruendemann, S.; Golubev, N. S.; Limbach, H. H. *Eur. J. Inorg. Chem.* **2001**, 1753−1761.
(51) Belkova, N. V.; Besora, M.; Epstein, L. M.; Lledós, A.; Maseras, F.; Shubina, E. S. *J. Am. Chem. Soc.* **2003**, *125*, 7715−7725.

Scheme 4

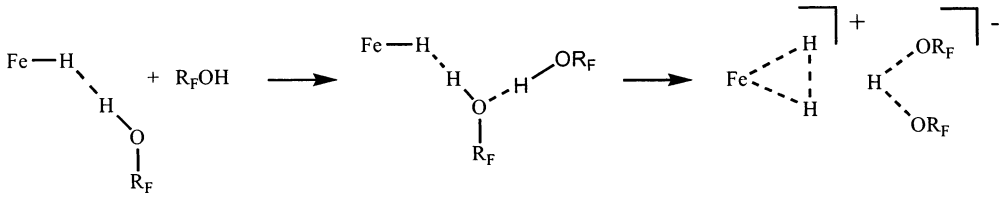

anism (pathway b in Scheme 2). The alternative possibility of reversible deprotonation followed by protonation at the metal center would certainly lead to a kinetics dependent on the nature of the acid.

It is interesting to compare our results with those reported for the related ruthenium systems (Ring)RuH(L)(L′) (Ring = Cp, Cp*; L,L′ = tertiary phosphine ligands).[6,29] For these, the occurrence of an intramolecular rearrangement mechanism leading from the dihydrogen complex to the dihydride isomer was proposed, in part, on the basis of the observation that the rate constant is invariant with the acid concentration. However, we have shown that this rate should not depend on the acid concentration even for a deprotonation/reprotonation mechanism (see Supporting Information). The observation by Chinn and Heinkey[6] that the isomerization is faster than H/D scrambling in the presence of external acids is much stronger evidence in favor of an intramolecular mechanism. Our observations, based on the comparison of isomerization rates in the presence of acids of different strength, are complementary and lead to the same conclusion for the related Fe system. In addition, however, they show the absence of a kinetically viable direct protonation of the metal site under the same experimental conditions in which the isomerization process occurs. For the previous studies carried out by Heinekey and Puerta on the hydridoruthenium complexes, as well as for the previous study by Hamon et al. on Cp*FeH(dppe), the proton-transfer process is carried out at very low temperature, where the direct protonation of the metal site may be disfavored by large negative activation entropies. Those studies, therefore, do not necessarily prove that a competitive metal protonation would not occur at ambient temperature.

Conclusion

The direct and independent observation, *at the same temperature*, of the kinetics for the faster protonation of the hydride ligand site in complex Cp*FeH(dppe) and for the isomerization of the resulting $Cp^*Fe(H_2)(dppe)^+$ intermediate to the thermodynamically preferred classical dihydride product has allowed us to obtain strong evidence in favor of a direct isomerization process, not involving the reversible deprotonation of the hydride site and protonation of the metal site. The unambiguous presence of a direct proton-transfer pathway to the metal site, for any complex which contains hydride ligands, remains to be established. Further investigations will be necessary to probe the generality or limitations of the results reported here.

Acknowledgment. This work was supported by the European Commission's RTN Program (HPRN-CT-2002-00176), by INTAS (00-00179), by RFBR (No. 02-03-32194, 03-03-6283), and by NATO (PST.CLG.978453).

Supporting Information Available: Derivation of equations for the observed rate constant of the tautomerization process under the two different mechanistic hypotheses (PDF). This material is available free of charge via the Internet at http://pubs.acs.org.

JA0358450